Colloids and Surfaces B: Biointerfaces 109 (2013) 45–51

Contents lists available at SciVerse ScienceDirect

Colloids and Surfaces B: Biointerfaces

journal homepage: www.elsevier.com/locate/colsurfb

Biosensor based on ds-DNA decorated chitosan modified multiwall carbon nanotubes for voltammetric biodetection of herbicide amitrole

Ali A. Ensafi*, Maryam Amini, Behzad Rezaei

Department of Chemistry, Isfahan University of Technology, Isfahan 84156-83111, Iran

ARTICLE INFO

Article history:
Received 8 November 2012
Received in revised form 10 March 2013
Accepted 26 March 2013
Available online 2 April 2013

Keywords:
Amitrole
DNA biosensor
Intercalative binding
Chitosan-modified multiwall carbon nanotubes
Voltammetry

ABSTRACT

The interaction of amitrole and salmon sperm ds-DNA was studied using UV–vis and differential pulse voltammetry (DPV) at both bare and DNA-modified electrodes. Amitrole showed an oxidation peak at 0.445 V at a bare pencil graphite electrode (PGE). When ds-DNA was added into the amitrole solution, the peak current of amitrole decreased and the peak potential underwent a shift. UV–vis spectra showed that the absorption intensity of the ds-DNA at 260 nm decreased with increasing amitrole concentration, proving the interaction between amitrole and the ds-DNA. The results also showed that amitrole could interact with the ds-DNA molecules via the intercalative binding mode. Finally, a pretreated pencil graphite electrode (PGE) modified with multiwall carbon nanotubes (MWCNTs) and chitosan (CHIT) decorated with the ds-DNA were tested in order to determine amitrole content in solution. Electrochemical oxidation of amitrole bonded on DNA/MWCNTs–CHIT/PGE was used to obtain an analytical signal. A linear dependence was observed to exist between the peak current and 0.025–2.4 ng mL^{-1} amitrole with a detection limit of 0.017 ng mL^{-1}. The sensor showed a good selectivity and precision for the determination of amitrole. Finally, applicability of the biosensor was evaluated by measuring the analyte in soil and water samples with good selectivity.

1. Introduction

Although pesticides have led to enhanced agricultural productivity in recent years, their release into the environment has made the problem of water quality a major concern at both national and international levels [1]. As required by the European Union, pesticide concentration in drinking water should not exceed 0.1 μg L^{-1} for each individual compound or 0.5 μg L^{-1} for total pesticides [2].

Amitrole [3-amino-1,2,4 triazol] is an herbicide wildly used in agricultural practices as a mixed formulation with other pesticides [3–5]. The Environmental Protection Agency (EPA) prohibited the use of amitrole in food crops due to its proven carcinogenetic effects on animals [6]. Moreover, its good solubility in water may lead to its leaching into the environment, thereby polluting both ground and surface waters [7]. The electrochemical biosensors are used as good tools for pollutants screening and detection as they are fast, simple and cost effective [8–10]. Different methods have been proposed in the literature for amitrole determination in water, using different analytical methods such as capillary electrophoreses [1,2,11], liquid chromatography [3,12], high performance liquid chromatography [7,13], and electrochemical methods [14–21]. Electrochemical biosensors are used as a good tool for pollutants screening and detection as they are fast, simple, and cost effective [11–13].

The study of the characteristics of carbon nanotubes (CNTs) has in recent years formed an impressive research field in electroanalytical applications. Their properties such as high electronic conductivity and high mechanical resistance have led to their use in the preparation of electrochemical sensors. Furthermore, the increasing active surface area of electrodes and the anti-fouling capacity of electrode surfaces upon modification with CNTs are among the important practical advantages of CNTs, especially with regards to electroanalytical chemistry [22–24]. Fabrication of CNT-based films using the layer-by-layer method (LBL) has attracted increasing attention because of their simplicity and the wide choice of materials available. For example, multilayer films of multiwall carbon nanotubes (MWCNTs) have been homogeneously and stably assembled on the surface of graphite electrodes using the LBL method, which is based on the electrostatic interaction between negatively charged CNTs and positively charged chitosan [25].

Nucleic acids are used as a powerful tool in identifying and monitoring many significant compounds [26]. Molecules and ions interact with DNA in three meaningfully different ways: namely, electrostatic, groove-binding, and intercalation. These reactions cause changes in the structure of DNA and the base sequence, leading to the perturbation of DNA replication. Electrostatic interactions, being usually non-specific, consist of binding along the exterior of the ds-DNA. Groove-binding interactions involve direct

* Corresponding author. Tel.: +98 311 3913269; fax: +98 311 3912350.
E-mail addresses: Ensafi@cc.iut.ac.ir, aaensafi@gmail.com (A.A. Ensafi).

0927-7765/$ – see front matter © 2013 Elsevier B.V. All rights reserved.
http://dx.doi.org/10.1016/j.colsurfb.2013.03.031

interaction of the compound with the edges of the base pairs in the major or minor grooves of ds-DNA. Having very high sequence specificity, they extend to fit over many base pairs. Intercalation encompasses inserting planar or nearly planar aromatic ring systems between the base pairs, causing unwinding and separation of base pairs. Drugs that intercalate into ds-DNA have been extensively studied, and the field has been recently reviewed using a variety of techniques. Electrochemical investigation of DNA–drug interaction can provide a simple and inexpensive method for the determination of drugs. To construct the electrochemical DNA–biosensors, nucleic recognition layer is immobilized over an electrochemical transducer. Changes in the DNA structure during intercalation with DNA binding are detected by nucleic acid recognition layer [27–29].

The high degree of reproducibility together with other benefits such as low cost, commercial accessibility, and ease of preparation are the main reasons for selecting the disposable pencil graphite electrode (PGE). To the best of our knowledge, electrochemical determination of amitrole based on its interactions with ds-DNA and the use of PGE has not yet been reported. In this study, a DNA biosensor was constructed and used for the determination of amitrole. For this purpose, a mixture of MWCNTs and chitosan was immobilized on the surface of a pretreated pencil graphite electrode (PGE) to improve the immobilization of ds-DNA on the surface. The signal of amitrole after interaction with the ds-DNA was used for constructing the calibration curve and ultimately for quantitative inspections. It was found that the interaction between ds-DNA and amitrole leads to the preconcentration of amitrole at the surface of the modified electrode and the improved detection limit of this method.

2. Materials and methods

2.1. Chemicals

All solutions were prepared using reagent grade chemicals, and doubly distilled water was used through the work. Amitrole was purchased from Aldrich Chemicals (Milwaukee, USA). Double-strand salmon sperm ds-DNA (ds-DNA, catalog no. D-8899) was purchased from Sigma (St. Louis, USA). Reagent grade Tris–HCl, CH_3COOH, CH_3COONa, HNO_3, EDTA, NaCl, $K_3Fe(CN)_6$, $K_4Fe(CN)_6$ and NaOH were purchased from Aldrich Chemicals (Milwaukee, USA).

A salmon sperm ds-DNA stock solution was prepared in Tris buffer (TE, pH 7.0) and kept frozen. More diluted solutions of the ds-DNA were prepared with acetate buffer solution (pH 4.8) containing 0.02 mol L^{-1} NaCl.

Stock solutions of amitrole were prepared by dissolving accurately weighed of amitrole. The solution was conserved at 4 °C, covered with aluminum foil and left to attain room temperature before use. Amitrole working solutions for voltammetric investigations were prepared by the dilution of the stock solution with the acetate buffer (pH 4.8) containing 0.01 mol L^{-1} NaCl. MWCNTs were purchased from Aldrich Chemicals (Milwaukee, USA).

Chitosan was obtained from Acros Chemical. The chitosan solution (0.5%) was prepared by dissolving 0.05 g chitosan in 10 mL CH_3COOH (2.0 mol L^{-1}) with the aid of sonication for 30 min. The chitosan solution was stored in refrigeration at 4 °C when not in use.

2.2. Apparatus

Electrochemical measurements were performed using an Autolab PGSTAT 12, potentiostat/galvanostat connected to a three-electrode cell, Metrohm Model 663 VA stand, with a GPES 4.9 software package (Eco Chemie, The Netherlands). The raw data was treated using the Savitzky and Golay filter (level 2) of the GPES software, followed by the GPES software moving average baseline correction with a "peak width" of 0.01. Differential pulse voltammetry with potential amplitude of 50 mV, a modulation time of 0.05 s, and a step potential of 8 mV was used.

Pencil graphite was obtained as a pencil lead composed of natural graphite, a polymeric binder and clay from Rotring Co. Ltd., Germany (R 505210 N, type 2B). The reference electrode was Ag/AgCl (3 mol L^{-1} KCl) and the counter electrode was a platinum wire.

Cyclic voltammogram of 5.0 mmol L^{-1} $K_3[Fe(CN)_6]/K_4[Fe(CN)_6]$ in 0.1 mol L^{-1} KCl was recorded from −0.20 to 0.60 V using a scan rate of 100 mV s^{-1}. The anodic to cathodic peak potential separation was evaluated.

Electrochemical impedance spectroscopy measurements were carried out in the presence of 5.0 mmol L^{-1} $K_3[Fe(CN)_6]/K_4[Fe(CN)_6]$ as a redox probe in 0.1 mol L^{-1} KCl at a polarization potential of 0.15 V in the frequency range of 0.005–10^5 Hz and with an amplitude of 10 mV.

UV–vis spectra were measured with a double beam spectrophotometer, Jasco Model V-750, using 1.0 cm quartz cells.

Metrohm pH-meter (Model 827) with a glass electrode (Corning) was used to measure the solution pH.

2.3. Functionalization and purification of MWCNTs

MWCNTs were purified and functionalized as described elsewhere [30]. A mass of 120 mg of MWCNTs was stirred in 10 mL of a 3 mol L^{-1} nitric acid solution for 20 h. The solid product was collected on a filter paper and washed several times with distilled water until the filtrate solution became neutral (pH 7.0). The obtained functionalized MWCNTs were then dried in an oven at 80 °C for 24 h. Nitric acid usually causes a significant destruction of carbon nanotubes and introduces –COOH groups at the ends or at the sidewall defects of the nanotubes structure.

2.4. Preparation of single-stranded DNA

To prepare single strain DNA, the ds-DNA was heated in water bath at 100 °C for 30 min and cooled in an ice bath immediately [31].

2.5. Preparation of the electrodes

The body of the pencil lead was tightly coated with Teflon band. Electrical contact with the lead was achieved by soldering a copper wire to the metallic holder of the working electrode. The pencil lead was then fixed vertically and immersed into a solution in which the contact was only achieved via the cross section of the electrode. The surface was finally polished on a weighing paper to a smoothed finish before each use.

The surface of PGE was pretreated by applying +1.80 V for 300 s in a quiescent solution of 0.5 mol L^{-1} acetate buffer containing 0.02 mol L^{-1} NaCl (pH 4.8). Then, 3.0 mg MWCNTs was dispersed into 1.0 mL of the chitosan solution. The mixture was sonicated for 3 h to obtain a homogeneous black suspension, which was sonicated for 15 min immediately before preparing the MWCNTs–chitosan films. PGEs were dipped into this composite for 30 min. Then, the electrode was washed with deionized water and dried. To prepare the DNA-modified electrode, the modified graphite electrode was immersed in the 1.0 mg mL^{-1} DNA solution (in 0.5 mol L^{-1} acetate buffer solution and 0.02 mol L^{-1} NaCl, pH 4.8) under stirring (200 rpm) for 10 min at room temperature (20 °C). The electrode was subsequently washed with the acetate buffer (0.5 mol L^{-1} at pH 4.8) for 5 s to remove the unbounded

ds-DNA on the electrode surface. This modified PGE was designated as ds-DNA/CHIT–MWCNTs/PGE.

2.6. Interaction of amitrole with ds-DNA

2.6.1. Interaction between ds-DNA and amitrole in solution

In order to inspect the interaction between amitrole and the ds-DNA, stock DNA and amitrole solutions were added into the phosphate buffer solution (0.1 mol L^{-1} at pH 7.4) to produce the required concentrations, and the mixture thus obtained was stirred for an adequate period of time. A freshly polished PGE was immersed into the mixture solution. Differential pulse voltammograms were recorded by applying an initial potential of 0.00 V and a final potential of +1.00 V.

2.6.2. Interaction between ds-DNA and amitrole at the ds-DNA-modified electrode

In order to inspect the interaction between amitrole and ds-DNA, the ds-DNA-modified PGE was immersed into a stirred (200 rpm) acetate buffer solution (pH 4.8) containing different concentrations of amitrole for 300 s in an open circuit system. After the accumulation step, the ds-DNA modified PGE was rinsed and placed in NaOH 0.01 mol L^{-1} and differential pulse voltammograms were recorded by applying an initial potential of 0.00 V and a final potential of +1.00 V.

2.7. Preparation of real samples

Water samples were collected using a routine technique and stored in polyethylene bottles. Tap water was sampled from our laboratory in the Department of Chemistry at Isfahan University of Technology, Isfahan. River water was obtained from different sites along the Zayandehroud River in Isfahan (Iran). The samples were then filtered (using Whatmann No. 45) prior to their analysis which was carried out in the first 48 h after their collection.

Soil samples were collected from the campus of Isfahan University of Technology. All the soil samples were air-dried and gently ground with a pestle and mortar to pass through a 1.0 mm sieve. The sieved samples were further dried in an oven at 35 °C until they reached a constant weight. 100 mL 0.01 mol L^{-1} KBr (in 80% CH_3OH in water) was added to 5 grams of the soil sample thus prepared. Then, the resulting mixture was sonicated for 5 min and transferred into a centrifuge bottle where it was centrifuged at 2000 rpm for 15 min before it was filtered. The centrifuging and filtration steps were repeated three times and filtrates were collected by the following procedures: (1) a certain amount of the filtrate was collected and added into 0.5 mol L^{-1} of the acetate buffer solution containing 0.02 mol L^{-1} NaCl at pH 4.8 to detect the analyte with the biosensor; and (2) the filtrate was nearly dried in a rotary evaporator at 80 °C and the residue was dissolved in water in order to detect the analyte using HPLC (Environmental Protection Agency (EPA) standard method) [32]. All the soil and water samples were stored at 4 °C. For the standard addition method, soil and water samples were prepared by adding amitrole prior to each treatment. Soil and water samples were spiked with a known amount of amitrole and recovery measurements were made.

3. Results and discussion

3.1. Characterization of the chitosan–MWCNTs film

MWCNTs are not soluble in water and acidic media due to the wander Waals attraction between nanotubes. After functionalization of MWCNTs, —COOH and —OH groups are created on the surface of MWCNTs. Chitosan is a cationic biopolymer which can absorb some anionic groups of the functionalized MWCNTs. So, MWCNTs can be dispersed in chitosan solution to improve their stability [33].

AFM is an excellent tool for studying the surface morphology of thin films on a micro-scale. Fig. 1 shows the AFM amplitude images of unmodified PGE, MWCNTs–CHIT modified PGE, and DNA/MWCNTs–CHIT modified PGE surfaces. The surface roughness of unmodified PGE is clearly seen in Fig. 1A. Randomly oriented carbon nanotubes could be seen from the AFM image of the obtained CHIT–MWCNTs layer (Fig. 1B). The MWCNTs are covered uniformly on the entire surface of the PGE. MWCNTs used in this work have a diameter of 70–110 nm and a length of 5–9 μm. Positively charged chitosan is easily coated on the negatively charged surface of the MWCNTs by electrostatic interaction. As a result, the nanotubes become "fat" to a diameter of about 600 nm (Fig. 1B). Chitosan molecules can combine considerably well with negatively charged DNA to form DNA films because it is a strong linear cationic polyelectrolyte. As shown in the AFM image (Fig. 1C), DNA molecules are aggregated and saturated on the CHIT–MWCNTs. The MWCNTs not only display unique electron transfer properties that induce the conductivity of chitosan and improve electron transfer characteristics, they also increase the amount of chitosan deposited on the electrode surface. Also, this demonstrates that chitosan can be used as a good matrix for MWCNTs and DNA. Chitosan acts as a polymer backbone, giving stable and homogeneous thin films.

The cyclic voltammogram (CV) of the $[Fe(CN)_6]^{3-/4-}$ system is widely used for monitoring the characteristics of the surface of modified electrodes. Fig. 2A demonstrates the CVs of the unmodified PGE, MWCNT–CHIT modified PGE, and DNA/MWCNT–CHIT modified PGE in 5.0 mmol L^{-1} $[Fe(CN)_6]^{3-/4-}$ redox probe containing 0.1 mol L^{-1} KCl. As can be seen, the anodic peak potential of $Fe(CN)_6^{3-/4-}$ at the unmodified PGE appeared at +0.35 V and the cathodic peak potential at 0.07 V vs. Ag/AgCl. After modification of the PGE with MWCNTs–CHIT mixture, the redox peak currents of $Fe(CN)_6^{3-/4-}$ increased, indicating that MWCNTs improved the electroactivity of the electrode. Furthermore, there was a significant change at the MWCNTs–CHIT redox peak potentials of $Fe(CN)_6^{3-/4-}$ as compared to the redox potentials obtained in the case of unmodified PGE due to the repulsion between the negative charge of the phosphate group of DNA and $Fe(CN)_6^{3-/4-}$. However, alternative current (AC) impedance spectroscopy was also used to identify the effect of the modification. Fig. 2B shows the impedance spectra of the unmodified PGE, MWCNT–CHIT modified–PGE, and DNA/MWCNT–CHIT modified PGE in 5.0 mmol L^{-1} $Fe(CN)_6^{3-/4-}$ (1:1) containing 0.1 mol L^{-1} KCl. Compared with the unmodified PGE, a smaller semi-circle at higher frequencies was observed at MWCNTs–CHIT/PGE. This indicated that the impedance of the electrode decreased obviously in the presence of the MWCNTs–CHIT nanocomposite which may have promoted the electron exchange between $Fe(CN)_6^{3-/4-}$ and the electrode. The charge transfer resistance, R_{ct}, indicating the diameter of the semicircle for DNA/MWCNTs–CHIT/PGE biosensor, is higher than that of the electrode without DNA because its negatively charged interface represents an electrostatic barrier toward the anions of the redox probe.

3.2. Interaction of amitrole with ds-DNA

Amitrole was electrochemically oxidized, which exhibited one anodic peak in the potential range under the potential range investigated (Fig. 3). Typical DPV behaviors of 1.5 ng mL^{-1} amitrole in the absence and presence of different concentrations of ds-DNA at pH 7.4 are shown in Fig. 3A. The anodic peak potential (E_{pa}) in the absence of ds-DNA is located at 0.65 V. Under the experimental conditions of Fig. 3, pure ds-DNA displays no electrochemical signals at the PGE. This is mainly due to the merging of the anodic peak at low ds-DNA concentrations and the background discharge [34]. As

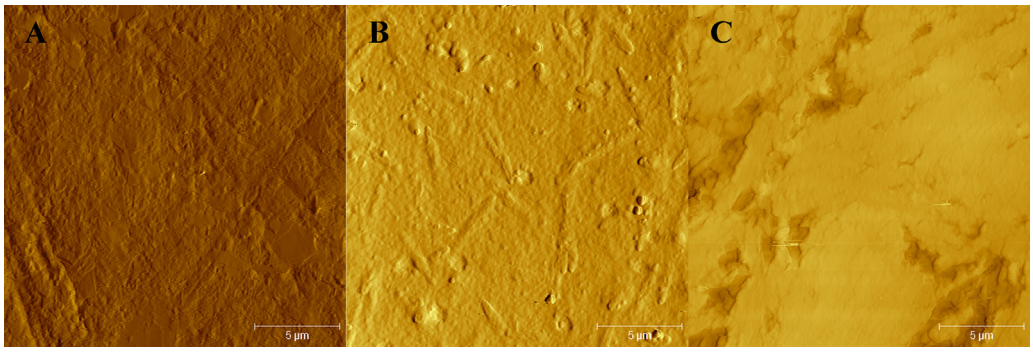

Fig. 1. AFM images of (A) unmodified PGE; (B) MWCNTs–CHIT modified PGE; and (C) DNA/MWCNTs–CHIT modified PGE.

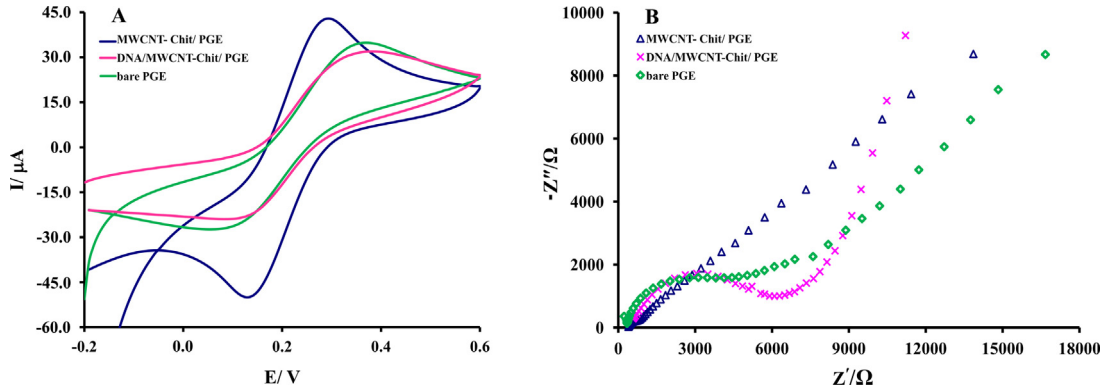

Fig. 2. A) CVs; and B) Impedance spectra of unmodified PGE, MWCNTs–CHIT/PGE and DNA/MWCNTs–CHIT/PGE in 5.0 mmol L^{-1} $Fe(CN)_6^{3-/4-}$ containing 0.1 mol L^{-1} KCl. CV measurement at scan rate of 100 mV s^{-1} between +0.20 and +0.60 V. (MWCNTs concentration: 3.0 mg mL^{-1}). Conditions: polarization potential: 0.15 V, frequency: 0.005 to 10^5 Hz, amplitude: 10 mV.

indicated by the DPV in Fig. 3A, the equilibrium concentration of amitrole in the presence of 5.0 μg mL^{-1} ds-DNA declines leading to a decrease in the peak current (I_p) with a positive shift of the anodic peak potential by 50 mV. Moreover, E_{pa} shifts to more positive potential and I_p obviously continues to decrease with increasing ds-DNA concentration (Fig. 3A). Base on these observations, it seems that the decreasing in the peak current of amitrole upon ds-DNA addition is due to the binding of amitrole with the bulky, slowly diffusing ds-DNA, which results in a considerable decrease in the apparent diffusion coefficient (D). As reported in the literature [35], the negatively shifted peak potential is characteristic of an electrostatic mode. If the peak potential shifts positively, the interaction will be an intercalative mode. It may, therefore, be claimed that amitrole is bound to DNA mainly through an intercalative mode.

Fig. 3B shows the differential pulse voltammetric (DPV) response of 1.5 ng mL^{-1} amitrole at both bare PGE and DNA/MWCNTs–CHIT/PGE. These studies were performed under open circuit conditions using 300 s as an accumulation time in 0.01 mol L^{-1} NaOH. Comparison of Fig. 3A and B reveals that the oxidation peak potential of amitrole has negatively shifted in the basic media. The plot of Ep vs. pH (Fig. 4A) shows a linear relationship in the pH range of 6–12. The magnitude of the slope of the line in Fig. 4A (ca. 56 mV/pH) indicates that one-electron (accompanied by one proton) oxidation process takes place on the electrode surface [17]. The peak current obtained at DNA/MWCNTs–CHIT/PGE was about 20 times higher than that obtained with the bare PGE. The positive shift of the peak potential and the increase in the peak current also indicated that amitrole could interact with the ds-DNA immobilized on the PGE surface. The results showed that the dsDNA-modified surface was more favorable for amitrol molecules to undergo redox reaction than the bare PG surface. This indicates a preconcentration of amitrole on the DNA-modified surface due to its binding to ds-DNA. The sharp anodic peak also indicates that amitrole underwent redox through the intercalated

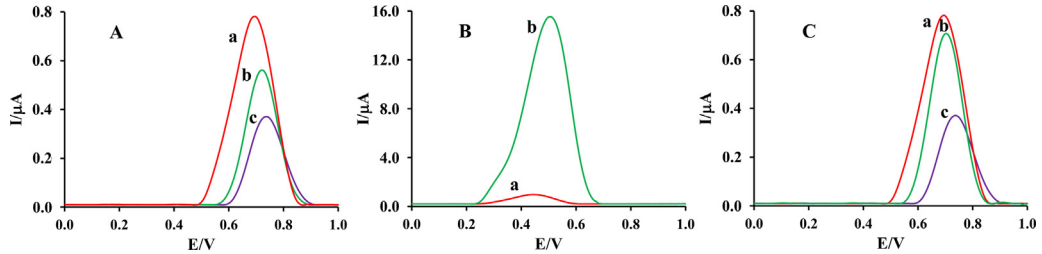

Fig. 3. (A) DPVs of 1.5 ng mL^{-1} amitrole at the unmodified PGE in phosphate buffer solution (0.1 mol L^{-1} at pH 7.4) with different concentrations of the ds-DNA: (a) 0.0 μg mL^{-1}, (b) 5.0 μg mL^{-1}, (c) 10.0 μg mL^{-1}. B) DPVs of 1.5 ng mL^{-1} amitrole in 0.01 mol L^{-1} NaOH solution at: (a) the unmodified PGE; and (b) DNA/MWCNTs–CHIT/PGE after 300 s as an accumulation time. C) DPVs of amitrole at the unmodified PGE in phosphate buffer solution (0.1 mol L^{-1} at pH 7.4); (a) 1.5 ng mL^{-1} amitrole; (b) 1.5 ng mL^{-1} amitrole and 10.0 μg mL^{-1} ss-DNA; and (c) 1.5 ng mL^{-1} amitrole and 10.0 μg mL^{-1} ds-DNA.

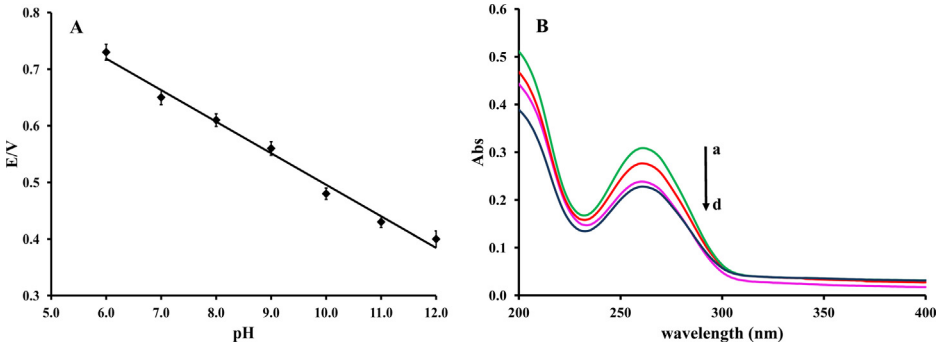

Fig. 4. (A) Dependence of oxidation peak potential of amitrole with pH at the unmodified PGE, (B) UV spectra of (a) 10.0 μg mL^{-1} ds-DNA; 10.0 μg mL^{-1} ds-DNA interacting with 1.0 μg mL^{-1} amitrole after (b) 2, (C) 5, and (d) 10 min in Tris buffer solution (pH 7.0). (The error bars are standard deviations for $n = 3$).

state. As the linear plot of I_p vs. ν (scan rate) revealed (figure not shown) that amitrole was strongly adsorbed at the surface of the modified electrode [36].

3.2.1. Comparison of the interactions of ds-DNA and ss-DNA with amitrole

In order to study the denaturation of natural DNA, 10 μg mL^{-1} of ds-DNA and 10 μg mL^{-1} of a ss-DNA were added into the phosphate buffer solution (0.1 mol L^{-1} at pH 7.4) containing 1.5 ng mL^{-1} amitrole, respectively, (at room temperature with stirring for 10 min) and DPV signals were recorded at the unmodified PGE. As shown in Fig. 3C, although the peak potentials were shifted positively and the peak currents decreased in both cases, the peak current of amitrole fell more sharply with ds-DNA. This demonstrated a more intense interaction of amitrole with ds-DNA, which might be the result of the higher intercalation binding nature between amitrole and ds-DNA or the increasing blockage of the electron transfer of amitrole through the electrode surface by ds-DNA absorption, or probably both. The distinct difference in DPV behaviors of amitrole could be used to distinguish ds-DNA from ss-DNA.

3.2.2. UV–vis spectra of interaction between amitrole and ds-DNA

Absorption spectrophotometry was used to prove the interaction between amitrole and ds-DNA. The absorption spectra of ds-DNA before and after interaction with amitrole are shown in Fig. 4B. A notable decrease in the absorbance of ds-DNA at 260 nm (interaction time is increased from 2 to 10 min) confirms the existence of an interaction between amitrole and ds-DNA and the results obtained from absorption spectrophotometry are a good proof of this interaction.

3.3. Selection of optimum experimental conditions for the preparation of the DNA biosensor

To construct DNA/MWCNTs–CHIT modified PGE, different variables such as immobilization time of MWCNTs–CHIT on PGE, amount of MWCNTs, incubation time of ds-DNA, and its concentration were optimized. In order to optimize the immobilization time of MWCNTs–CHIT, the pretreated PGEs were dipped into the MWCNTs–CHIT composite for 10, 20, 30, 40, 50, and 60 min. The results showed that a dramatic increase occurred in the oxidation peak currents of $Fe(CN)_6^{3-/4-}$ during the immobilization time up to min 30 after which the currents were almost leveled off over longer immobilization times. So, 30 min was selected as the immobilization time of MWCNTs and chitosan on PGE.

To check the influence of the amount of MWCNTs on the sensitivity of the MWCNTs–CHIT composite, the MWCNTs content in MWCNTs–CHIT composite was varied between 0.5 to 4.0 mg mL^{-1}. The results showed that the oxidation peak current of $Fe(CN)_6^{3-/4-}$ increased with increasing MWCNTs content up to 3.0 mg mL^{-1}, but decreased beyond that. Therefore, 3.0 mg mL^{-1} of MWCNTs suspension was selected and used in all further experiments.

The optimum conditions for the ds-DNA concentration and incubation time were studied to obtain the maximum guanine signal. To find the optimum concentration of ds-DNA, different concentrations of ds-DNA were used at the open circuit potential using 10 min as an incubation time. The results showed that the guanine signal increased by increasing ds-DNA concentration up to 1.0 mg mL^{-1}, beyond which it leveled off. Therefore, 1.0 mg mL^{-1} of salmon sperm ds-DNA was selected as the optimum concentration.

To find the optimum incubation time, different times were selected and studied at the open circuit potential using 1.0 mg mL^{-1} ds-DNA. DPV signals of guanine increased up to min 10 of the experiments but leveled off afterwards. Therefore, 10 min was considered as the optimum incubation time.

3.4. Optimal reaction conditions

In order to analyze amitrole, such variables as accumulation time and the pH levels of the interaction and measurement medium were optimized. Different pH levels in acidic media (pH < 6) were studied to find the optimum pH of the sample solution for the accumulation of the analyte at the electrode surface. For this purpose, the ds-DNA–modified PGE was immersed into a stirred (200 rpm) acetate buffer solution (pHs < 6) containing 1.5 ng mL^{-1} amitrole for 300 s in an open circuit system. After the accumulation step, the ds-DNA modified PGE was rinsed and placed in NaOH 0.01 mol L^{-1}. Finally, differential pulse voltammograms were recorded and the oxidation peak current of amitrole was checked. The results showed that pH 4.8 (acetic acid-acetate) was the best. This is due to the fact that in an acidic solution, the analyte has a positive charge which causes it to be adsorbed (electrostatically) at the negative charges (from DNA) present at the electrode surface.

In the second stage, the effect of the pH level of the measurement medium on signal sensitivity was investigated. Oxidation of amitrole at the surface of the modified electrode occurred in an alkaline solution. Therefore, the influence of the electrolyte pH on the response of DNA/MWCNTs–CHIT/PGE to amitrole (1.5 ng mL^{-1}, after 180 s accumulation time) was studied. The results showed that the maximum signal was observed at pH ≥ 12. Therefore, pH 12 (0.010 mol L^{-1} NaOH) was selected as the optimum pH for the analysis of amitrole throughout the work. It should be noted that this short scanning time of recording voltammograms (10 s) is not sufficient for denaturing ds-DNA [37].

The binding of amitrole to ds-DNA depends on the interaction (incubation) time. Thus, the incubation time for the

Table 1
Comparison of the efficiency of previously electrochemical studies in the determination of amitrole.

Electrode	Technique	Dynamic range (ng mL^{-1})	Limit of detection (ng mL^{-1})	Reference
MWCNTs/CPE	AdSV[a]	67.3–588.6	50.5	[12]
Modified CPE	Amperometry	200.0–2000.0	90.0	[13]
GCE	SWV[b]	42.0–21,020	32.0	[16]
Au	Amperometry	50.0–40,000.0	30.0	[18]
DNA/MWCNTs–CHIT/PGE	DPV	0.025–2.400	0.017	This work

[a] Adsorptive stripping voltammetry.
[b] Square wave voltammetry.

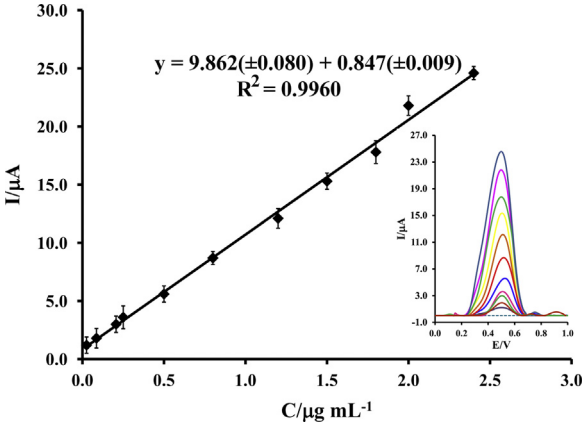

Fig. 5. Calibration curve for the determination of amitrole based on preconcentrated oxidation signal of amitrole at DNA/MWCNTs–CHIT/PGE. Inset: DPVs of (from top to down) 2.4, 2.0, 1.8, 1.5, 1.2, 0.80, 0.50, 0.25, 0.20, 0.085, 0.025, and 0.00 ng mL^{-1} amitrole (The error bars are standard deviations for $n = 3$).

interaction of amitrole with the DNA/MWCNTs–CHIT/PGE surface was optimized. The electrochemical detection was assessed and found to be in the range of 60–360 s as the incubation time of amitrole under an open circuit condition with stirring (200 rpm). The results showed that the interaction time increased up to 360 s, there was a dramatic increase in the oxidation signal of amitrole up to s 300, beyond which it was almost leveled off. Accordingly, 300 s was selected as the optimum time for the interaction of amitrole with the DNA/MWCNTs–CHIT/PGE.

4. Figures of merit

Fig. 5 shows the DPV peaks current for the intercalated amitrole as a function of its concentration in the exposure solution. The preconcentration process was accomplished by stirring (at 200 rpm) in the acetate buffer solution (pH 4.8) containing different concentrations of amitrole for 300 s in an open circuit system. The peak current increased linearly with amitrole concentration over the range of 0.025 to 2.4 ng mL^{-1} in 0.01 mol L^{-1} NaOH solution (Fig. 5). Saturated adsorption was attained with concentration higher than 2.4 ng mL^{-1}. A slope of 9.862 ± 0.080 μA mL ng^{-1} with a regression coefficient of 0.9980 was also obtained. The limit of detection (3 s) was estimated at 0.017 ng mL^{-1}. The value of the detection limit obtained for amitrole in this study is better than those reported in other electrochemical studies (Table 1).

5. Interference study

Interference studies were carried out using several species prior to the application of the proposed biosensor for the assay of amitrole in real samples. The potential interfering substances were chosen from the group of substances commonly found with amitrole in environmental and drinking water. Tolerance limit was defined as the maximum concentration of the potential interfering substance that caused an error less than 3% for the determination of amitrole concentration. The results showed that 1000-fold of SO_4^{2-}, CO_3^{2-}, NO_3^-, IO_4^-, SCN^-, ClO_3^-, $S_2O_3^{2-}$, I^-, Br^-, F^-, atrazine, ametryn, atraton, 2-hydroxyatrazine, 600-fold of Ca^{2+}, Mg^{2+}, and 300-fold of Fe^{3+}, Al^{3+}, Zn^{2+}, Cu^{2+}, NH_4^+, Cd^{2+}, Zn^{2+}, Ni^{2+} did not affect selectivity. The obtained data showed that the proposed method is selective for amitrole determination. The selectivity of the DNA/MWNT–CHIT/PGE for measuring amitrole is due to the weak interaction of the other substances with ds-DNA under the selected conditions.

6. Real sample analysis

To test the practical application of the biosensor developed here for the analysis of amitrole in real samples, environmental water (Zayandehroud River), tap water and soil samples were used. In cases where the concentration of amitrole was out of the linearity range, the soil sample solution was accurately diluted with

Table 2
Recovery of amitrole in water and soil sample using DNA/MWCNTs–CHIT/PGE.

Sample	Amitrole added	Amitrole found[a]	Recovery%	RSD%	EPA standard method [29]
Zayandehrood River water	–	<Limit of detection	–	–	<Limit of detection
	1.00 (ng mL^{-1})	1.04 (ng mL^{-1})	104.0	3.2	1.02 ± 0.06 (ng mL^{-1})
	2.00 (ng mL^{-1})	1.96 (ng mL^{-1})	98.0	2.6	–
Agricultural waste water	–	<Limit of detection	–	–	<Limit of detection
	1.00 (ng mL^{-1})	0.96 (ng mL^{-1})	96.0	3.0	0.94 ± 0.07 (ng mL^{-1})
	2.00 (ng mL^{-1})	2.07 (ng mL^{-1})	104.0	3.2	–
Drinking water	–	<Limit of detection	–	–	<Limit of detection
	1.00 (ng mL^{-1})	1.01 (ng mL^{-1})	101.0	2.4	0.97 ± 0.06 (ng mL^{-1})
	2.00 (ng mL^{-1})	2.03 (ng mL^{-1})	102.0	2.0	–
Soil sample	–	<Limit of detection	–	–	<Limit of detection
	14.0 (μg g^{-1})	13.2 (μg g^{-1})			13.4 ± 0.8 (μg g^{-1})
	20.0 (ng g^{-1})	18.8 (ng g^{-1})			–

[a] Average of four replicate measurements.

the buffer solution (0.5 mol L^{-1} acetate buffer solution containing 0.02 mol L^{-1} NaCl at pH 4.8). As a reference, the assayed samples were also studied using the EPA standard method as described in Section 2.7. The results for 4-time parallel measurements are presented in Table 2. Clearly, the good agreement found between the results from the proposed sensor and those obtained from the EPA method [29] indicate that the proposed biosensor was capable of efficiently determining amitrole in water and soil samples. Most importantly, the procedure of sample analysis is greatly simplified by the amitrole biosensor compared with EPA standard method as it is associated with a lower detection time and less possible errors caused due to the complex procedures of EPA method. Thus, the proposed method could be successfully applied for amitrole assay in soil and water samples without any interference.

7. Conclusion

Highly sensitive biosensors for the determination of herbicides in the environment and in drinking waters are particularly interesting. In the present study, a sensitive DNA–biosensor was developed for the determination of amitrole in water and soil samples. In this paper, the interaction of amitrole with ds-DNA was initially investigated using electrochemical and UV–vis spectroscopy. The results revealed an interaction between amitrole and ds-DNA. Chitosan as a polycation and MWCNTs of small sizes provide a surface with positive charges and a high surface area for the immobilization of ds-DNA as a polyanion. Using the DNA/MWCNTs–CHIT/PGE electrode, we were able to detect the interaction of amitrole with ds-DNA, which allowed us to apply a DNA-modified electrode for ultra-trace determination of amitrole. Amitrole can be preconcentrated in immobilized ds-DNA due to the intercalation in the double helix of the ds-DNA, which increases the differential pulse oxidation wave of amitrole 20-time higher than that of the bare electrode. This means that amitrole achieved a preconcentration 20 times higher than that when it could reach in the absence of ds-DNA. This finding can be applied for the determination of trace amounts of amitrole in the environment and in drinking waters. The advantages of the proposed method include its extremely low detection limits, wide linear dynamic range, and suitability for online and in situ measurements. Moreover, this method is fast, simple, sensitive, selective, and cost effective for the identification and evaluation of amitrole.

Acknowledgement

The authors wish to thank the Iran National Science Foundation (INSF) for their support (project no. 91047481).

References

[1] M. Chicharro, M. Moreno, E. Bermejo, S. Ongay, A. Zapardiel, J. Chromatogr. A 1099 (2005) 191.
[2] M. Chicharro, A. Zapardiel, E. Bermejo, M. Moreno, Talanta 59 (2003) 37.
[3] M. Girod, C. Delaurent, L. Charles, R. Commun, Mass Spectrom 20 (2006) 892.
[4] M.A. Fontecha-Camara, M.V. López-Ramón, L.M. Pastrana-Martínez, C. Moreno-Castilla, J. Hazard. Mater. 156 (2008) 472.
[5] S. Nader, C.J. Swanton, A.S. Hamill, J.D. Vyn, P.H. Sikkema, Weed Biol. Manag. 8 (2008) 139.
[6] M. Moreno, E. Bermejo, A. Sánchez, M. Chicharro, A. Zapardiel, Anal. Bioanal. Chem. 391 (2008) 867.
[7] Y. Sun, P. FeiLio, D. Wang, J. Qiang Li, Y. Song Cao, J. Agric. Food Chem. 57 (2009) 4540.
[8] S. Takeda, K. Fukushi, K. Chayama, Y. Nakayama, Y. Tanaka, Sh. Wakida, J. Chromatogr. A 1051 (2004) 297.
[9] I. Bobeldijk, K. Broess, P. Speksnijder, T. van Leerdam, J. Chromatogr. A 938 (2001) 15.
[10] Y. Sun, L. Luo, F. Wang, J. Li, Y. Cao, Anal. Bioanal. Chem. 395 (2009) 465.
[11] F. Lucarelli, A. Kicela, I. Palchetti, G. Marrazza, M. Mascini, Bioelectrochemistry 58 (2002) 113.
[12] K. Kerman, B. Meric, D. Ozkan, P. Kara, A. Erdem, M. Ozsoz, Anal. Chim. Acta 450 (2001) 45.
[13] L. Wu, X. Lu, J. Jin, H. Zhang, J. Chen, Biosens. Bioelectron. 26 (2011) 4040.
[14] J.M. Zen, H.P. Chen, A. Senthil Kumar, Anal. Chim. Acta 449 (2001) 95.
[15] M. Chicharro, E. Bermejo, M. Moreno, A. Sanchez, A. Zapardiel, G. Rivas, Electroanalysis 17 (2005) 476.
[16] M. Chicharro, A. Zapardiel, E. Bermejo, M. Moreno, E. Madrid, Anal. Bioanal. Chem. 373 (2002) 277.
[17] M. Siswana, K. Ozoemena, T. Nyokong, Talanta 69 (2006) 1136.
[18] M. Siswana, K. Ozoemena, T. Nyokong, Sensors 8 (2008) 5096.
[19] J.M. Zen, A. Senthil Kumar, M.R. Chang, Electrochim. Acta 45 (2000) 1691.
[20] T. Mugadza, T. Nyokong, Electrochim. Acta 55 (2010) 2606.
[21] F. Sanchez Bayo, R.V. Hyne, K.L. Desseille, Anal. Chim. Acta 675 (2010) 125.
[22] A. Merkoc, M. Pumera, X. Llopis, B. Perez, M. del Valle, S. Alegret, TRAC 24 (2005) 826.
[23] J. Wang, Analyst 130 (2005) 421.
[24] G.G. Wildgoose, C.E. Banks, H.C. Leventis, R.G. Compton, Microchim. Acta 152 (2006) 187.
[25] L. Agui, P. Yanez Sedeno, J.M. Pingarron, Anal. Chim. Acta 622 (2008) 11.
[26] E. Mirmomtaz, A.A. Ensafi, S. Soleimanian-Zad, Electrochim. Acta 54 (2009) 1141.
[27] E. Mirmomtaz, A.A. Ensafi, Electrochim. Acta 54 (2009) 4353.
[28] A.A. Ensafi, E. HeydariBafrooei, M. Amini, Biosens. Bioelectron. 31 (2012) 376.
[29] A.A. Ensafi, B. Rezaei, M. Amini, E. Heydari Bafrooei, Talanta 88 (2012) 244.
[30] M.E. Ghica, R. Pauliukaite, O. Fatibello Filho, C.M.A. Brett, Sens. Actuators B 142 (2009) 308.
[31] L. Wang, H. Xiong, X. Zhang, Sh. Wang, Electrochem. Commun. 11 (2009) 2129.
[32] EPA, MRID 436468-01: A High Performance Liquid Chromatographic Method for Measurement of Amitrole Residue in Soil, US Environmental Protection Agency, Cincinatti, OH, 1993.
[33] J. Li, Q. Liu, Y. Liu, Sh. Liu, Sh. Yao, Anal. Biochem. 346 (2005) 107.
[34] M.S. Ibrahim, Anal. Chim. Acta 443 (2001) 63–72.
[35] M.T. Cater, A.J. Bard, J. Am. Chem. Soc. 109 (1987) 7528.
[36] A.J. Bard, L.R. Faulkner, Electrochemical Methods: Fundamentals and Applications, John Wiley & Sons, New York, 1980.
[37] M. Ageno, E. Dore, C. Frontali, The alkaline denaturation of DNA, Biophys. J. 9 (1969) 1281.